

Structural And Morphological Properties Of (Ns. Bc/ ZnO)Bio-Composite Adsorption

Hanane Rehali^{1,2}, Hayet Menasra^{1,3}, Sihem Djebabra^{1,4}, Amel Aidi^{1,5}, Fedia Bekiri⁶, Chaima Benbrika⁷, Hamida Khadidja^{1,8}

^{1,4}Industrial chemistry Department, University of Biskra (07000), Algeria

^{2,5,8} Laboratory of LARGHYDE, University of Biskra Bp 145 RP, Biskra 07000, Algeria

^{3,7} Applied chemistry laboratory, material science faculty, University of Biskra (07000), Algeria

⁶ Scientific and Technical Center Research on Arid Regions, University of Biskra (07000), Algeria

The Author's Email: h.rahali@univ-biskra.dz^{1,2}, h.menasra@univ-biskra.dz³, s.djebabra@univ-biskra.dz⁴, a.aidi@univ-biskra.dz⁵, sandi_elamel@yahoo.fr⁶, chaima.benbrika@univ-biskra.dz⁷, khadija.hamida@univ-biskra.dz⁸

Received: 03/08/2023

Published: 05/11/2023

Abstract

The synthesis in a single step from charcoal nut shells (Ns) to obtain a novel Ns. Biochar/ ZnO bio-composite. The chemical activation of the Bio-carbon with a solution of ZnCl₂ at 0.136 mole and neutral pH to give a pure composite at T=600 °C which is characterized by scanning electron microscope (SEM), x ray diffraction (DRX) and spectroscopy Fourier transform-infrared (FTIR) and UV-Visible spectroscopy to study adsorption of copper ions. The adsorption kinetic appropriate to the Experimental data is the pseudo-second order model kinetic. The experimental adsorption capacity for copper ions is 1273 mg/g at temperature 20°C. Thus, the low-cost synthesis of the ZnO Bio-composite is a promoter axis for the adsorption of copper ions.

Keywords-biochar, kinetic models, adsorption, isotherm, Nut shells, copper.

Tob Regul Sci.™ 2023 ;9(2): 929 - 949

DOI: doi.org/10.18001/TRS.9.2.57

1. Introduction

The Industrial activities are very important sources of environmental pollution, which contains many heavy metal ions such as Cu²⁺, Zn²⁺, Ni²⁺, Ca²⁺ and Pb²⁺ ions are widely distributed in the

environment and these ions are very important for life and very toxic to living organisms including human beings [1]. In particular, Cu^{2+} is an important metal ion present in the effluents of industries. However, Cu^{2+} ion is dangerous to human health treatment process used to treat pollutants for Cu^{2+} ions, photo catalytic degradation, oxidation, biological degradation strategies [2, 3], filtration, extraction, reduction and bio-adsorption. Bio-adsorption method is a very good process to deal with removed Cu^{2+} ion contamination from wastewater because it is not expensive technology than other methods and less harmful to the environment [4]. Biochar have made substantial breakthroughs in reducing greenhouse gas emissions and global warming, reducing soil nutrient leaching losses, sequester atmospheric carbon into the soil, increasing agricultural productivity, reducing bioavailability of environmental contaminants and subsequently, becoming a value-added product sustaining bio-economy. Bio-economy implies the exploration and exploitation of bio-resources, which involves the use of biotechnology to create new bio-products of economic value. Biochar is a marketable bio-product, which can be used in agriculture, industries and energy sector [5].

In recent years, the ease of modification of Biochar by metal oxides has attracted the attention of several researchers to improve the adsorbent properties of pollutants [6]. For example, adding MnO to biochar facilitates the removal of Pb (II) and Cd (II) ions [7]. However, if iron oxide is added in parallel with magnesium oxide and Biochar to form the composite (Mg/ Fe-LHD biochar), this increases the co-adsorption of cations and anions [8].

Originality of this work, we studied the adsorption of Cu^{2+} ions solution to use a raw nut shells obtained from Algeria to produce the nut shells biochar is abbreviated (Ns. BC). This bio-carbon was prepared in a single step and low synthesis with chemical activation using zinc chloride solution at $\text{ZnCl}_2=0.136$ mole and a neutral pH at temperature $T=600^\circ\text{C}$ to give a pure composite (Ns.BC/ ZnO). The novel biochar/ ZnO composite has been characterized and applied to structural properties surface functional groups.

In this work we studied many parameters to effect from copper adsorption like stirring time, mass bio-product (Ns.BC/ ZnO) composite and initial concentration of copper(II) ions effect. All adsorption tests were conducted at neutral pH. The experimental adsorption capacity at equilibrium (Q_e) calculated with the isothermal and kinetic models.

2. Experimental

The different measuring devices used are:

- X-ray diffraction (XRD) analysis of the biochar/ ZnO composite was carried out on an equipped name in the two angle ranging from 5° to 80° .
- Fourier transforms infrared (FTIR) spectroscopy measurements using 6700 FTIR technique Spectrometer over the wave range from 4000 to 400 cm^{-1} .

- Spectroscopy UV-Visible using Shimadzu model.
- pH meter using HANNA pH 210 model with a combination electrode (Bioblock Scientific).
- EDS technique “Tescan Vega 3” was used for surface morphology and elemental analysis of the prepared material.
- SEM The Scanning electron microscopy illustrates the surface physical morphology of pure bio-composite biochar/ ZnO.

The raw material was used as an adsorbent, we prepared from the nut shells from Algeria to the production of pure composite. The cleaning with distilled water several times raw material (nut shells) to remove all impurities. Next step is drying in an oven at 105 °C for night. After, pre-carbonization at 200 °C for six hours to allow the elimination of the rest of the impurities. After cooling of the nut shells from the carbonized put in an electric grinder in order to obtain homogeneous materials for the needs of laboratory studies. The grinding time depends on the mass to be ground at 15-20 min. The sizes of the particles used for the adsorption tests were mechanically isolated using vibrating electric sieves whose mesh size corresponds to diameters $X_p=0.2$ mm. We mix 20 g raw charcoal with zinc chloride solution at $m_{ZnCl_2}=18,53g$ to activated bio carbon and keep stirring for half hour. The mixture putted in an oven for ten hours at 105 °C. The product placed in the same muffle furnace up to 600 °C for 4 hours and maintained at this temperature for one and a half hours (1.5) then cooled in the open air. We prepared stock solutions with a concentration of copper $10g.l^{-1}$ of distilled water using copper sulfate ($Cu(SO_4)$). Then we diluted in different proportions to prepare solutions of lower concentrations used in our tests.

Adsorption tests were carried out discontinuously at 293 K (except for temperature effect experiments) and studied three repetitions of the same experiment. In 250 ml Erlenmeyer flasks containing copper ions solution at a specified concentration, 1g (Ns.BC/ ZnO) adsorbent was introduced. The mixtures were stirred at a speed of 200 rpm for the desired time. The solutions were then filtered through a 0.45 μm membrane filter and the residual copper ions content was detected by a UV-vis spectrophotometer (Shimadzu model) at 810 nm. In the isotherm study, copper solutions with concentrations ranging from 1 to 8g/l were used at a constant temperature (~293 K)

Percent metal removal (%) [9-11] and adsorption capacity at equilibrium (Q_e) [12-18] were calculated by equations listed in table 1

Table 1: Equations of the different isotherm and kinetic models

Equation	formula	SYMBOLS AND UNITS
	$\% = \frac{(C_i - C_e)}{C_i} \times 100$	%: rate copper (II) removal
	$Q_e = (C_0 - C_e) \times \frac{V}{m}$	Q_e : adsorption capacity at equilibrium(mg/g) C_0 : initial concentration of Cu^{2+} ions (g/l)
Freundlich	$\ln Q_e = \ln KF + \frac{1}{n} \ln C_e$	C_e : equilibrium concentration of adsorbent in solution(g/l).
Langmuir	$\frac{1}{Q_e} = \left(\frac{1}{K_L Q_0} \right) \times \left(\frac{1}{C_e} \right) + \frac{1}{Q_0}$	V : volume of solution (l) m : mass of the adsorbent use(g) . n : constant related to the adsorption intensity.
	$R_L = \frac{1}{1 + K_L \times C_0}$	

<p>Temkin</p> $Q_e = B \ln K_t + B \ln C_e$ $B = \frac{RT}{\Delta Q}$ $R = 8.314 \text{ J. mol}^{-1} \cdot \text{K}^{-1}$	<p>Q_o: maximum capacity adsorption (mg/g)</p> <p>K_L : Langmuir isotherm equilibrium constant (l/mg)</p> <p>R_L: indicates the conformational property of the isotherm</p> <p>K_t: Temkin isotherm equilibrium constant (l/g)</p> <p>ΔQ: variation in adsorption energy (J/mole)</p> <p>Q_t: the adsorption capacity at time (t) (mg/g)</p> <p>R: universal ideal gas constant (J/mol. K).</p> <p>T: absolute temperature (K)</p>
<p>Kinetic first order</p> $\ln (Q_e - Q_t) = \ln Q_e - k_1 t$	<p>k₁: the constant of pseudo first order kinetic model (1/min)</p>
<p>Kinetic second order</p> $\frac{t}{Q_t} = \left(\frac{1}{Q_e^2 k_2} \right) + \frac{t}{Q_e}$	<p>k₂: constant of the pseudo second-order adsorption (g/ (mg.min))</p> <p>R²: correlation coefficient</p>

Intraparticle diffusion	$Q_t = K_{int} t^{1/2} + C$	k_{int} : constant of intra particle diffusion model (mg/g.min ^{-1/2})
-------------------------	-----------------------------	--

3. Result and Discussion

Fig.1 displays the identification of functional groups within the adsorbent (walnut shells) used in this research at two different temperatures: 20 °C and 200 °C. A broad band located at [3050-3670] cm⁻¹ is likely attributed to the (O-H) vibration of water molecules [10]. In the spectral range between 2914 cm⁻¹ and 2851 cm⁻¹, we observed vibrations related to the (C-H) asymmetrical stretching, which can be attributed to the presence of methyl/methylene groups [12-16]. The vibration associated with the aromatic (C = C) ring stretching of lignin was identified at 1602 cm⁻¹ [13-17]. The absorption bands at 1390 cm⁻¹ can be attributed to aromatic skeleton vibrations combined with (C-H) in-plane deformations of biochars [8], as well as the aromatic C-O and phenolic O-H stretching due to the presence of cellulose, hemicellulose, and lignin [8-13] at 1089 cm⁻¹.

Additionally, Fig. 2 reveals the appearance of two novel bands assigned to (Zn-O) at 703 cm⁻¹ and (O-Zn-O) at 993 cm⁻¹, indicating stretching vibration groups [19].

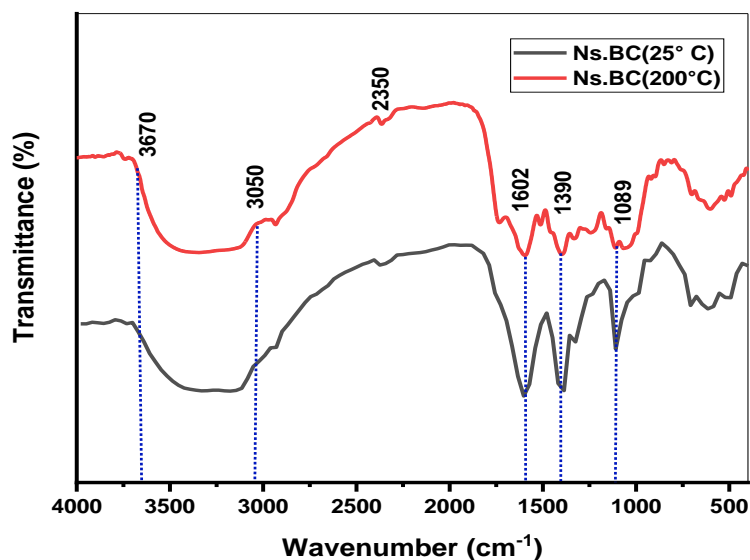


Fig.1.FTIR Spectrum of Ns.BC.

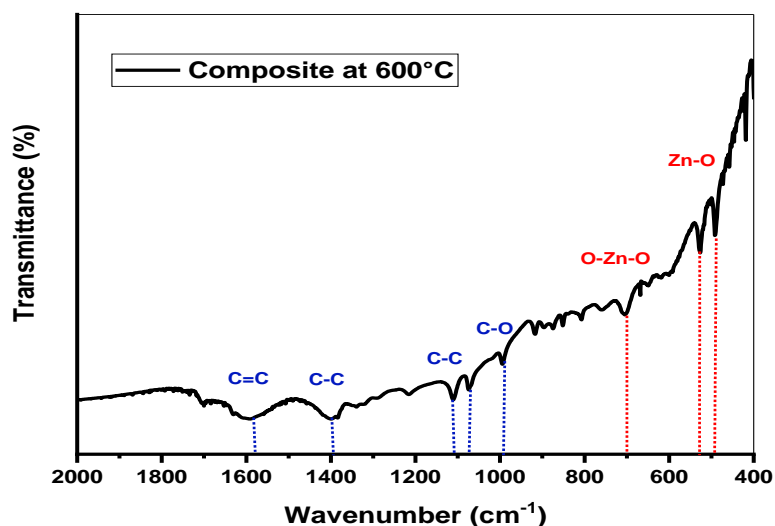
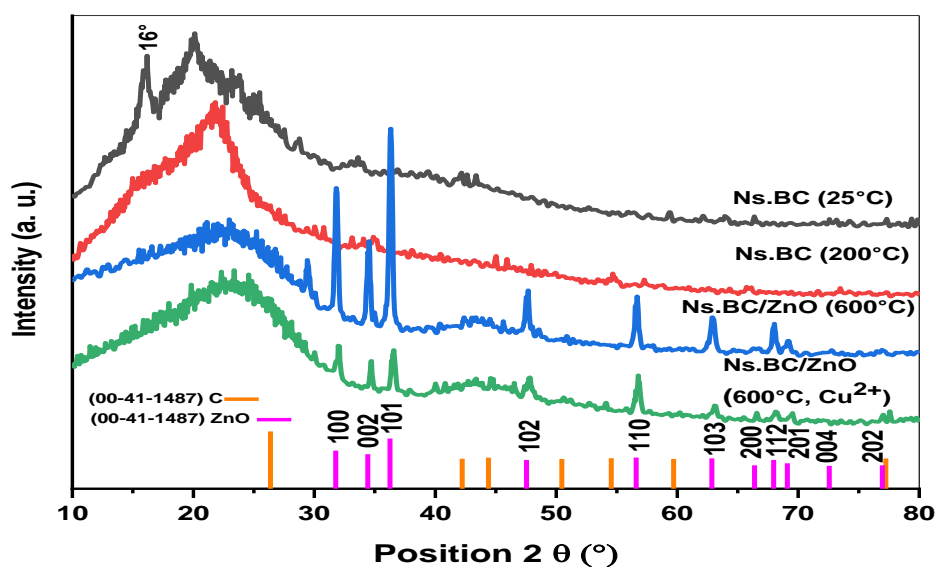


Fig.2. FTIR Spectrum of Ns.BC/ ZnO bio-composite

We used X-ray diffraction (XRD) technology to detect the crystalline aspect of our precursor and (Ns.BC/ ZnO) composite under the influence of temperature. All the results of the structural analysis (DRX) presented in Fig 3.



e

Fig.3.XRD Patterns of Ns.BC and (Ns.BC/ ZnO) bio-composite.

The spread reflection of the (002) and (101) planes in the vicinity of ($2\theta = 24^\circ$) and ($2\theta = 40^\circ$) suggests a low crystallinity in the formed biochar, confirming its amorphous carbon structure as per JCPDS no. (00-41-1487) [20-22]. However, a sharp peak at 16° corresponding to the (110) plane of cellulose I_β is observed in calcined nutshells [23].

The activation of carbon in a molar solution of ZnCl₂ at a neutral pH and a temperature of 600°C results in a robust insertion of ZnO with a single hexagonal wurtzite structure. The X-ray

diffraction (XRD) pattern shows the presence of crystalline planes (100), (002), (101), (102), (110), (103), (200), (112), (201), (004), and (202) at 2θ positions of 31.83° , 34.5° , 36.31° , 47.64° , 56.65° , 62.95° , 66.49° , 68.0° , and 69.17° , respectively, identical to JCPDS no. (00-36-1451).

The equation of the formation of ZnO :

Δ



600 °C

Additionally, the size of ZnO crystallites, calculated using the Debye–Scherrer equation ($D_{\text{sch}} = (k \times \lambda) / (\beta \cos(\theta))$) [22, 23], where $k = 0.9$ is the shape factor and β is the full width at half maximum, is 32.3 nm, and it increases to 39.7 nm after adsorption. This confirms the formation of a heterojunction between the biochar structure and the ZnO crystallites in the presence of copper ions.

Fig 4. (a and b) shows SEM images of (Ns.BC) and (Ns.BC/ ZnO) bio-composite. The two previous compounds were chosen for the morphological study because (Ns.BC) formed at 200 °C is a support of zinc oxide molecules. Both materials appear to have an irregular and porous structure, which is similar to the results (Ying Wang et al., 2020)[24] who used nut shells biochar as a precursor. **Fig4. (2b)** shows (Ns.BC/ ZnO) bio-composite that has more open pores than none activate biochar. These results indicate that the process of simultaneous activation and insertion of ZnO on the surface is effective in reducing the H₂O molecules of the carbon pore structure [25].

The micrograph of **Fig 4. (b1)** shows that size ZnO aggregations vary from 1.84 μm to 5.4 μm.

Moreover, **fig 4 (d and e)** present EDS spectrum and atom weight ratio of Ns.BC and Ns.BC/ ZnO bio-composite. The results shows that all the elements Carbon(C), Oxygen(O) and Zinc(Zn) are uniformly dispersed and without impurities. According to the studies of Sajjadi et al. [25] and Chen et al. [26], the good aggregation of ZnO particles on the biochar support is due to its high carbon content and low oxygen content.

Fig5. indicated that the removal of copper (%) on (Ns.BC/ZnO)bio-composite decreased gradually with an increase in the initial concentration of Cu²⁺ions. At low concentrations, the copper ions had a large number of available adsorption sites[27]. However, at the higher initial concentration of copper ions solution, the competition of Cu²⁺ ions for adsorption sites of the Ns.BC/ ZnO adsorbent becomes important.

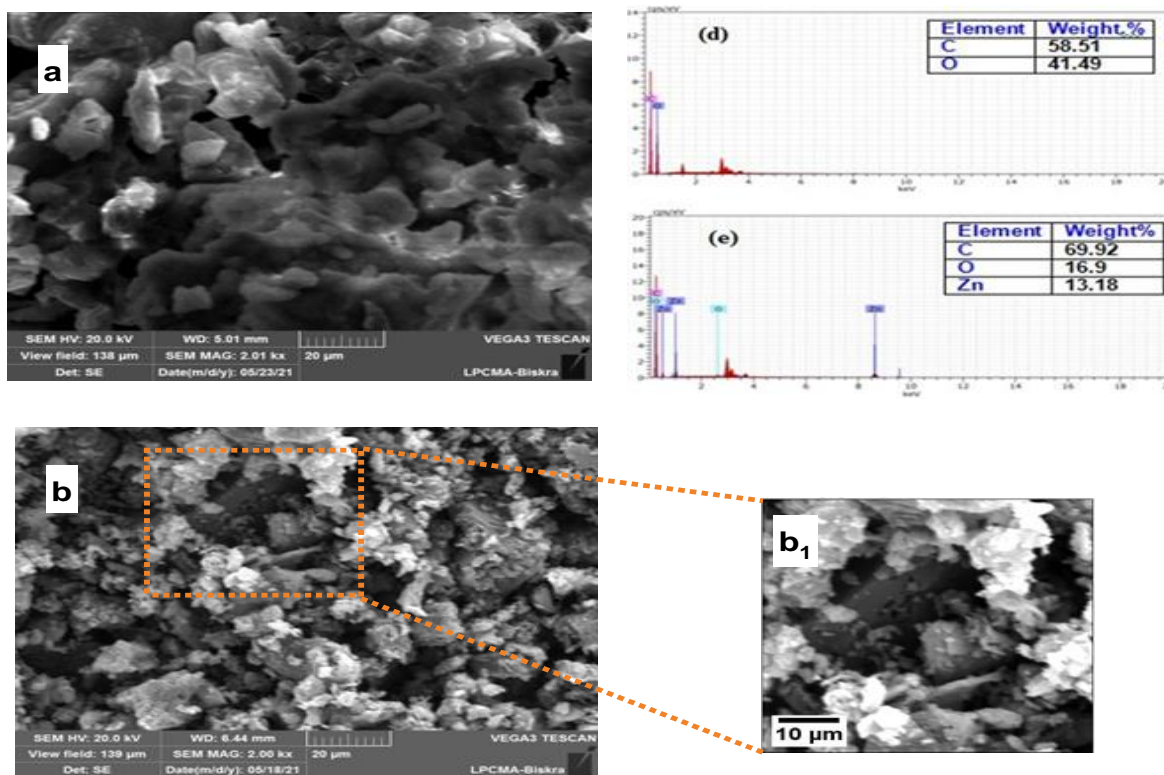


Fig. 4. SEM image of (a) Ns.BC (b) Ns.BC/ ZnO (d) EDS of Ns.BC (e) EDS of Ns.BC / ZnO bio-composite.

As a result, each unit mass of adsorbent is subjected to higher amounts of Cu^{2+} ions. The adsorption sites became saturated, and no more sites were available for further sorption. Therefore, the adsorption of Cu^{2+} on Ns.BC/ ZnO composite is dependent on the initial Cu^{2+} ion concentration [27, 28].

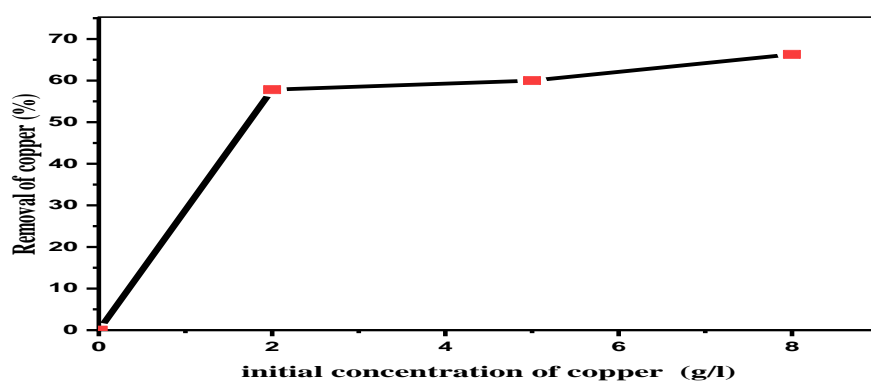


Fig. 5. Initial concentration effect on amount Cu^{2+} ions adsorbed ($v = 200 \text{ rpm}$, $T = 20 \text{ }^\circ\text{C}$) using a pure bio-composite (Ns.BC/ ZnO)

Results Fig. 6. showed that the adsorption of Cu^{2+} ions occurred in two stages, where in the initial

phase goes up quickly. This is attributed to the high number of available free sites for adsorbing the Cu^{2+} ions molecules [27, 28]. With in sixty minutes, the capacity of copper (II) adsorption about (1273 mg/g) of the total Cu^{2+} ions concentration (8 g/l). After ninety minutes a gradual decrease in the speed of the adsorption process is noted, where copper ions slowly occupy the remaining active sites due to the saturation adsorbent surface [29-31].

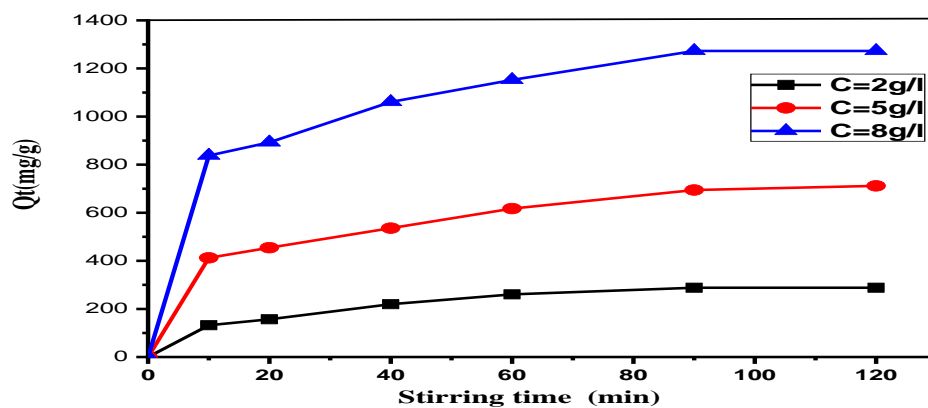


Fig. 6. Stirring time effect on amount of Cu^{2+} adsorbed ($v=200\text{rpm}$, $T=20^\circ\text{C}$) using a pure bio-composite (Ns.BC/ ZnO)

The adsorption removal efficiency increased with the adsorbent dose (Fig7). This phenomenon can be attributed to the increased dose of Ns.BC/ ZnO adsorbent, resulting in an increase in the availability of active sites on the surface of each biochar. However, these adsorption sites remained unsaturated during the adsorption reaction. These results have been previously reported in other studies that investigated the influence of variations in the adsorbent dose on the adsorption of copper ion [27, 32].

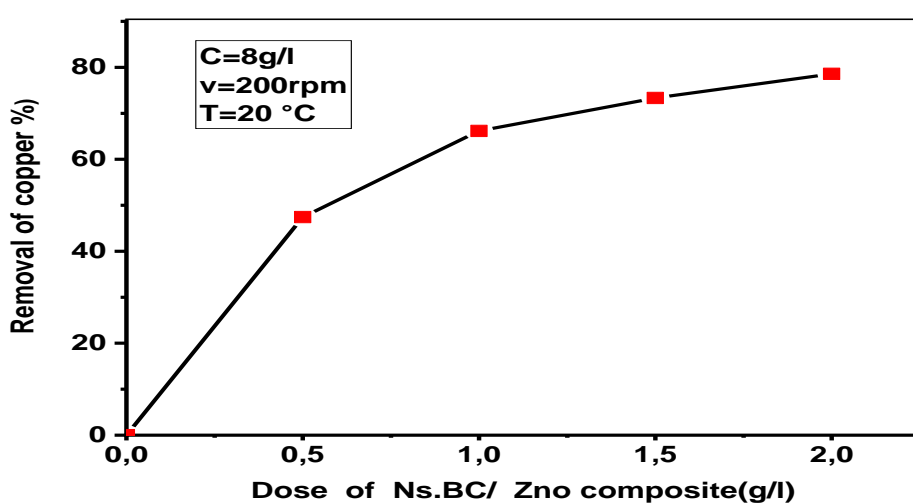


Fig.7. Effect of dosage (Ns.BC/ ZnO) bio-composite on removal Cu^{2+} ions

Fig.8 demonstrate the value of n was much greater than 1, there was a considerably strong interaction between Cu^{2+} and Ns.BC/ ZnO adsorbent became the adsorption process was inclined to take place [16].

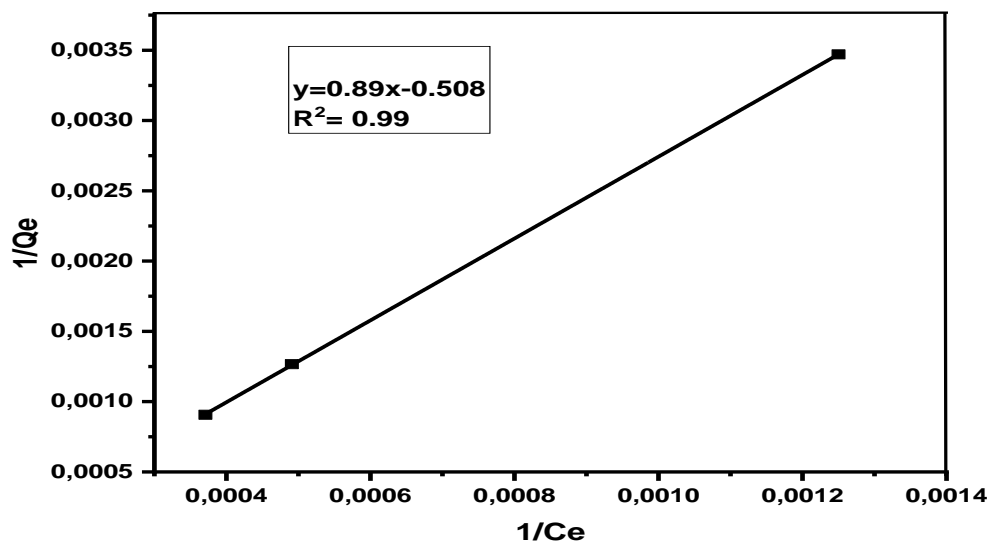


Fig.8. Freundlich isotherm on removal Cu(II) ions using (Ns.BC/ ZnO) bio-composite.

Comparison of fitting the Langmuir isotherm [33] is thermo -equation on the Cu^{2+} ions adsorption by a pure (Ns.BC/ ZnO) composite carried out at $T= 20\text{ }^\circ\text{C}$ and stirring speed 200rpm. Fig 9. shown a good fit of Langmuir isotherm were estimated $R^2=0.999$. The results of this model are listed in Table (2).

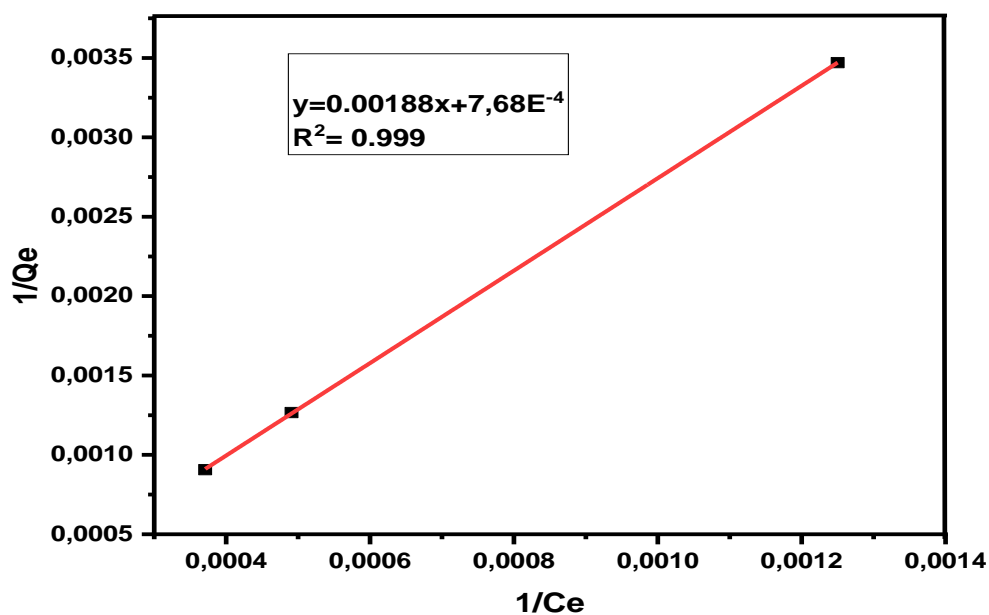


Fig.9.Langmuir isotherm on removal Cu^{2+} ions using (Ns.BC/ ZnO)bio-composite.

From this research work, the value of separation factor were calculated $R_L = 0.75$ indicating that the equilibrium adsorption was favorable and it showed that the value of R^2 of the Langmuir isotherm was higher than that of Temkin model proving that the adsorption data fitted well to Langmuir isotherm. This indicated that the adsorption process was a mainly monolayer bonding process occurring in specific heterogeneous binding sites [34].

The following values were estimated: $\Delta Q = 3.4 \frac{J}{mol}$ which is an indication of the heat of adsorption indicating a chemical adsorption process and the value R^2 obtained from the Temkin model [35-37] were less comparable to those obtained from the Freundlich and Langmuir isotherms.

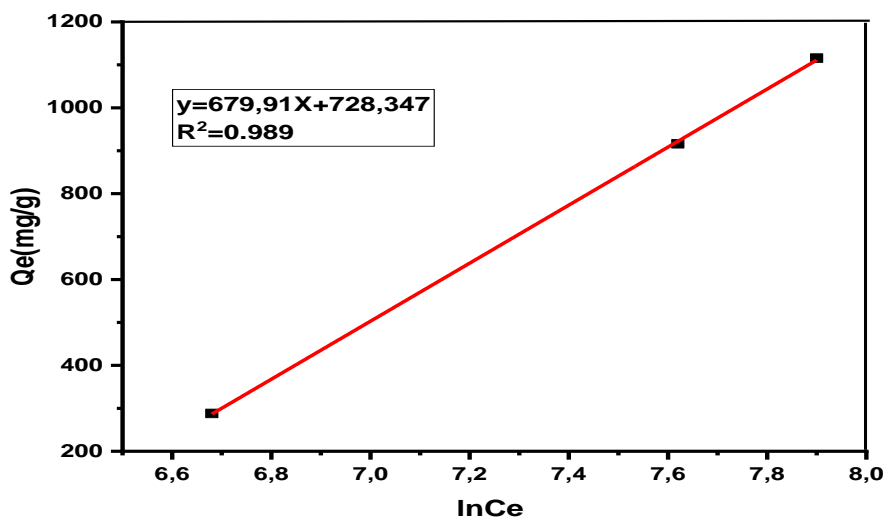


Fig.10.Temkin isotherm on removal Cu (II)ionsusing Ns.BC/ZnO bio-composite

Table2: Parameters of isotherm models

Models	Parameters	units	Values
	R ²	-	0.99
	Kf	L /g	0.601
Freundlich	n	-	1.12
	R ²		0.999
	Q ₀	mg/g	1302
	R _L		0.75
Langmuir	K _l	l/g	0.408
	R ²	-	0.98
Temkin	K _t	l/g	2.91
	ΔQ	J/mol	3.34

The pseudo first order kinetic model (Fig.11) were explained by Lagergren [38, 39] equation listed in table 1. The pseudo second-order kinetic [38], which is described by the chemical

reactionsThe pseudo second-order Kinetic modelshowing that the R^2 value was almost 1 as well plot than pseudo-first order kinetic model. These results are seen in Table3.

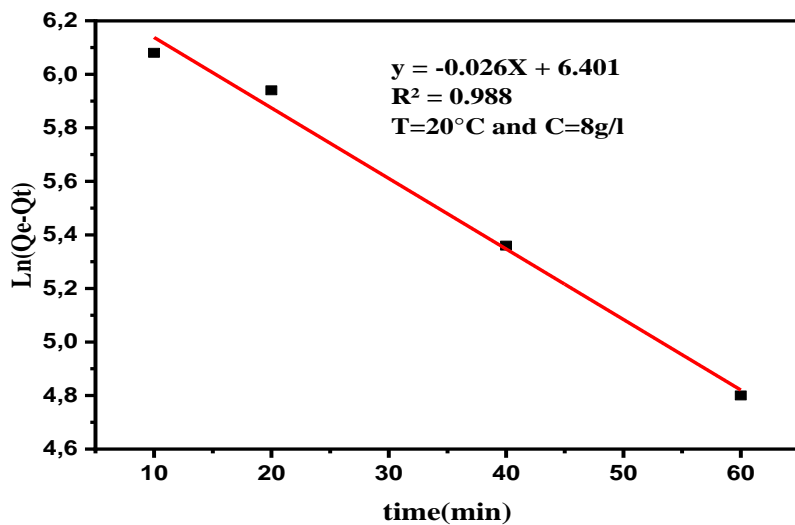
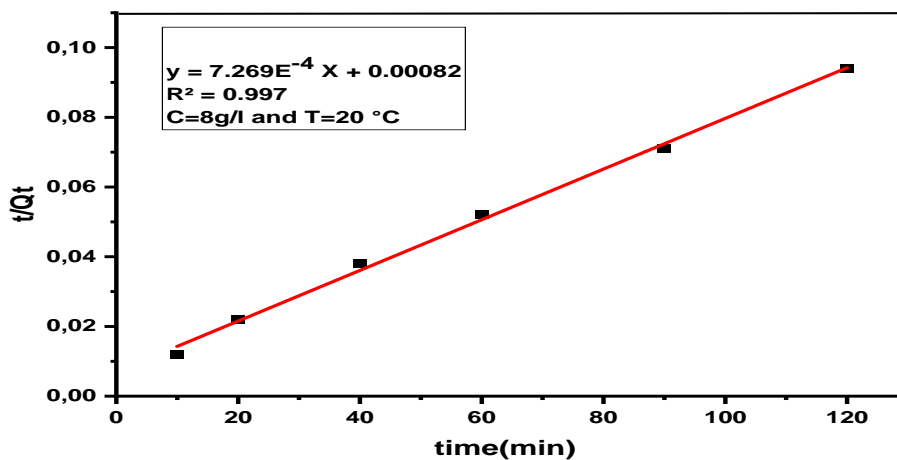


Fig.11. Pseudo first order Kinetic on removal Cu^{2+} ions using (Ns.BC/ ZnO) bio- composite.



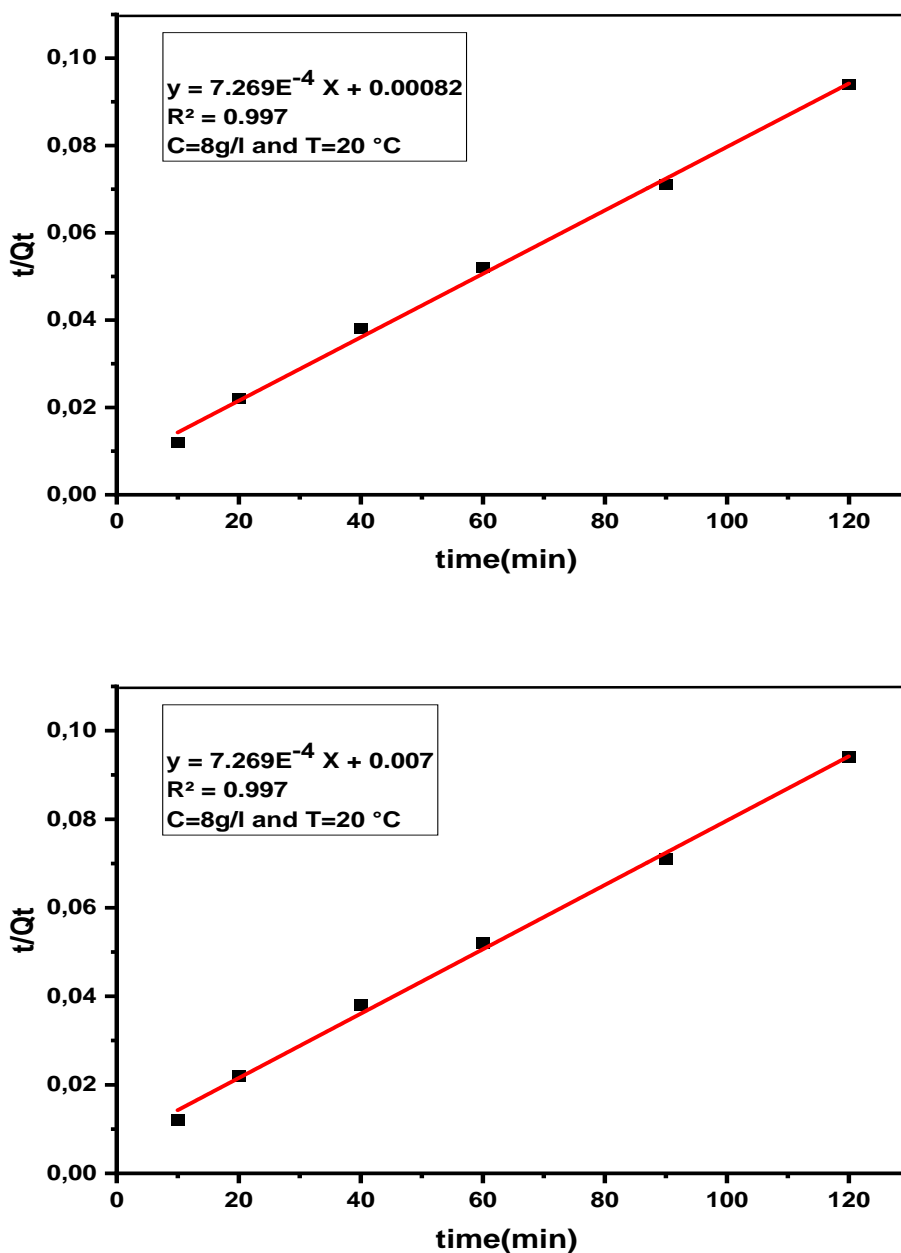


Fig.12. Pseudo second kinetic model to removal Cu^{2+} ions using (Ns.BC/ ZnO) bio-composite.

The intraparticle diffusion equation expressed as Weber and Morris [38] listed in table 1.

Fig.11, Fig.12 and Fig.13 shown three models plots, the constants (k_1 , k_2 , K_{int}) and Q_e were determined using the slope and intercept of these plots, respectively. The experimental results of the parameter of the three models kinetic were calculated and listed in Table 3, the pseudo second order kinetic model well plot with a R^2 value close to 1.

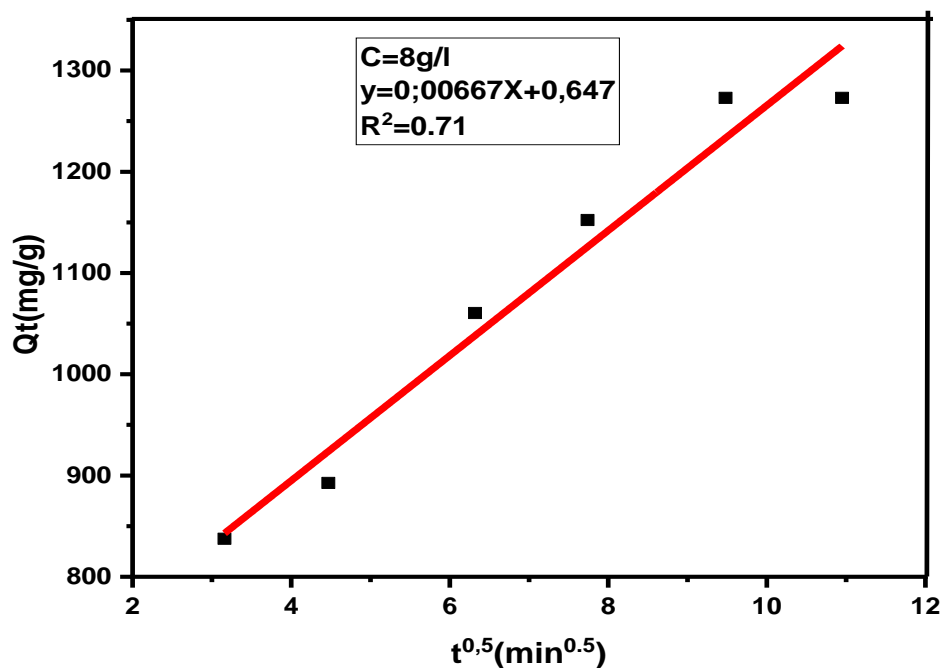


Fig.13. Intra-particle diffusion model on removal Cu²⁺ions using (Ns.BC/ ZnO) bio-composite

Table3: Parameters of order Kinetic models for adsorption copper (II) using Ns.BC/ZnO bio-composite.

Models	Parameters	units	Values
Pseudo first order	R ²	-	0.989
	K ₁	min ⁻¹	0.026
	Q _e	mg/g	602
Pseudo second order	R ²	-	0.99
	K ₂	g/mg.min	0.00092
	Q _e	mg/g	1220
	R ²	-	0.716

	K_{int}	(mg/g.min ^{0.5})	0.00667
Intraparticle diffusion	C	-	0.647

4. Conclusion

We used nut shells biomass as low-cost adsorbent in the treatment of waste water. This raw material can be characterized by DRX, MEB and FTIR. The step of carbonized NS-biochar at T=600°C and the activation with zinc chloride solution to give a pure bio-composite (Ns. BC/ ZnO). The FTIR spectrum of (Ns.BC) confirmed two novel peaks assigned to (Zn-O) at 703cm⁻¹ and (O-Zn-O) at 993cm⁻¹ stretching vibrations group. This bio-composite (Ns.BC/ZnO) is good adsorbent to eliminate Cu (II) ions solution. The kinetic of adsorption Cu (II) ions can be fitted well by Pseudo-second-order model. The maximum adsorption capacity for Cu (II) ions was calculated Q=1273 mg/g at 20°C. The stability of the (Ns. BC/ ZnO) bio-composite and its good morphological properties allowed good adsorption of copper ions in polluted waters, which paved the way for its application to other heavy metals threatening the environment.

References

1. Ghogomu, J., S. Mulu, D. Ajifack, A. Alongamo, and D.J.I.J.A.C. Noufame, *Adsorption of lead (II) from aqueous solution using activated carbon prepared from raffia palm (Raphia hookeri) fruit epicarp*. 2016. **9**(7): p. 74-85.
2. Cui, H., M. Fu, S. Yu, and M.K.J.J.o.h.m. Wang, *Reduction and removal of Cr (VI) from aqueous solutions using modified byproducts of beer production*. 2011. **186**(2-3): p. 1625-1631.

3. Døssing, L., K. Dideriksen, S. Stipp, and R.J.C.g. Frei, *Reduction of hexavalent chromium by ferrous iron: A process of chromium isotope fractionation and its relevance to natural environments*. 2011. **285**(1-4): p. 157-166.
4. Ossman, M., M. Mansour, M. Fattah, N. Taha, and Y.J.B.C.C. Kiros, *Peanut shells and talc powder for removal of hexavalent chromium from aqueous solutions*. 2014. **46**: p. 629-639.
5. Oni, B.A., O. Oziegbe, and O.O.J.A.o.A.S. Olawole, *Significance of biochar application to the environment and economy*. 2019. **64**(2): p. 222-236.
6. Liu, M., E. Almatrafi, Y. Zhang, P. Xu, B. Song, C. Zhou, G. Zeng, and Y.J.S.o.t.T.E. Zhu, *A critical review of biochar-based materials for the remediation of heavy metal contaminated environment: Applications and practical evaluations*. 2022. **806**: p. 150531.
7. Liang, J., X. Li, Z. Yu, G. Zeng, Y. Luo, L. Jiang, Z. Yang, Y. Qian, H.J.A.S.C. Wu, and Engineering, *Amorphous MnO₂ modified biochar derived from aerobically composted swine manure for adsorption of Pb (II) and Cd (II)*. 2017. **5**(6): p. 5049-5058.
8. Zhang, L., S. Tang, C. Jiang, X. Jiang, Y.J.A.a.m. Guan, and interfaces, *Simultaneous and efficient capture of inorganic nitrogen and heavy metals by polyporous layered double hydroxide and biochar composite for agricultural nonpoint pollution control*. 2018. **10**(49): p. 43013-43030.
9. Sireesha, S., U. Upadhyay, I.J.B.C. Sreedhar, and Biorefinery, *Comparative studies of heavy metal removal from aqueous solution using novel biomass and biochar-based adsorbents: characterization, process optimization, and regeneration*. 2022: p. 1-13.
10. Sharma, P.J.B.T., *Efficiency of bacteria and bacterial assisted phytoremediation of heavy metals: an update*. 2021. **328**: p. 124835.
11. Sharma, P. and S.J.B.T. Kumar, *Bioremediation of heavy metals from industrial effluents by endophytes and their metabolic activity: Recent advances*. 2021. **339**: p. 125589.
12. Marković, S., A. Stanković, Z. Lopičić, S. Lazarević, M. Stojanović, and D.J.J.o.E.C.E. Uskoković, *Application of raw peach shell particles for removal of methylene blue*. 2015. **3**(2): p. 716-724.
13. Naima, A., F. Ammar, O. Abdelkader, C. Rachid, H. Lynda, A. Syafiuddin, and R.J.B.t. Boopathy, *Development of a novel and efficient biochar produced from pepper stem for effective ibuprofen removal*. 2022. **347**: p. 126685.
14. Alfattani, R., M.A. Shah, M.I.H. Siddiqui, M.A. Ali, and I.A.J.E. Alnaser, *Bio-char characterization produced from walnut shell biomass through slow pyrolysis: sustainable for soil amendment and an alternate bio-fuel*. 2021. **15**(1):

p. 1.

15. Xu, F., J. Yu, T. Tesso, F. Dowell, and D.J.A.e. Wang, *Qualitative and quantitative analysis of lignocellulosic biomass using infrared techniques: a mini-review*. 2013. **104**: p. 801-809.
16. Spagnoli, A.A., D.A. Giannakoudakis, and S.J.J.o.M.L. Bashkova, *Adsorption of methylene blue on cashew nut shell based carbons activated with zinc chloride: The role of surface and structural parameters*. 2017. **229**: p. 465-471.
17. Ammar, F., C. Rachid, A. Amel, and A.J.I.J.o.C.T. Naima, *Kinetics and Isotherms modeling of methylene blue adsorption by Black Carbon using the shells of apricot kernels*. 2022. **28(4)**: p. 412-420.
18. Duy Nguyen, H., H. Nguyen Tran, H.-P. Chao, and C.-C.J.W. Lin, *Activated carbons derived from teak sawdust-hydrochars for efficient removal of methylene blue, copper, and cadmium from aqueous solution*. 2019. **11(12)**: p. 2581.
19. Cao, Q., Y. Zhang, J. Chen, M. Zhu, C. Yang, H. Guo, Y. Song, Y. Li, J.J.I.c. Zhou, and products, *Electrospun biomass based carbon nanofibers as high-performance supercapacitors*. 2020. **148**: p. 112181.
20. Carraro, P.S., L. Spessato, L.H. Crespo, J.T. Yokoyama, J.M. Fonseca, K.C. Bedin, A. Ronix, A.L. Cazetta, T.L. Silva, and V.C.J.J.o.M.L. Almeida, *Activated carbon fibers prepared from cellulose and polyester-derived residues and their application on removal of Pb²⁺ ions from aqueous solution*. 2019. **289**: p. 111150.
21. Zhang, L., T. Liu, N. Chen, Y. Jia, R. Cai, W. Theis, X. Yang, Y. Xia, D. Yang, and X.J.J.o.M.C.A. Yao, *Scalable and controllable synthesis of atomic metal electrocatalysts assisted by an egg-box in alginate*. 2018. **6(38)**: p. 18417-18425.
22. Nishiyama, Y., P. Langan, and H.J.J.o.t.A.C.S. Chanzy, *Crystal structure and hydrogen-bonding system in cellulose I β from synchrotron X-ray and neutron fiber diffraction*. 2002. **124(31)**: p. 9074-9082.
23. de Freitas, N.L., J.P. Coutinho, M.C. Silva, H.L. Lira, R.H.G.A. Kiminami, and A.C.F. de Melo Costa. *Synthesis of Ni-Zn ferrite catalysts by combustion reaction using different fuels*. in *Materials Science Forum*. 2010. Trans Tech Publ.
24. Wang, Y., L. Wang, X. Deng, H.J.E.S. Gao, and P. Research, *A facile pyrolysis synthesis of biochar/ZnO passivator: immobilization behavior and mechanisms for Cu (II) in soil*. 2020. **27**: p. 1888-1897.
25. Sajjadi, S.-A., A. Meknati, E.C. Lima, G.L. Dotto, D.I. Mendoza-Castillo, I. Anastopoulos, F. Alakhras, E.I. Unuabonah, P. Singh, and A.J.J.o.E.M. Hosseini-

- Bandegharaei, *A novel route for preparation of chemically activated carbon from pistachio wood for highly efficient Pb (II) sorption*. 2019. **236**: p. 34-44.
26. Chen, W., J. Meng, X. Han, Y. Lan, and W.J.B. Zhang, *Past, present, and future of biochar*. 2019. **1**: p. 75-87.
27. YOUCEF, L.J.I.J.o.C.T., *Optimization of process conditions to improve copper adsorption capacity of raw and treated Algerian bentonite: Characterization, kinetics and equilibrium study*. 2021. **28**(3): p. 249-261.
28. Mousavi, H.Z., A. Hosseinifar, and V.J.J.o.t.S.C.S. Jahed, *Removal of Cu (II) from wastewater by waste tire rubber ash*. 2010. **75**(6): p. 845-853.
29. Rahmati, A., A. Ghaemi, and M.J.A.o.N.E. Samadfam, *Kinetic and thermodynamic studies of uranium (VI) adsorption using Amberlite IRA-910 resin*. 2012. **39**(1): p. 42-48.
30. Liu, B. and Y.J.J.o.M.C. Huang, *Polyethyleneimine modified eggshell membrane as a novel biosorbent for adsorption and detoxification of Cr (VI) from water*. 2011. **21**(43): p. 17413-17418.
31. Amer, M.W. and A.M.J.A.J.o.C. Awwad, *Removal of Zn (II), Cd (II) and Cu (II) Ions from Aqueous Solution by Nano-Structured Kaolinite*. 2017. **29**(5).
32. Langmuir, I.J.J.o.t.A.C.s., *The adsorption of gases on plane surfaces of glass, mica and platinum*. 1918. **40**(9): p. 1361-1403.
33. Hull, M.S., P.J. Vikesland, and I.R.J.A.t. Schultz, *Uptake and retention of metallic nanoparticles in the Mediterranean mussel (*Mytilus galloprovincialis*)*. 2013. **140**: p. 89-97.
34. Khan, T.A., M. Nazir, I. Ali, and A.J.A.J.o.C. Kumar, *Removal of chromium (VI) from aqueous solution using guar gum–nano zinc oxide biocomposite adsorbent*. 2017. **10**: p. S2388-S2398.
35. Ghaedi, M., M.N. Biyareh, S.N. Kokhdan, S. Shamsaldini, R. Sahraei, A. Daneshfar, S.J.M.S. Shahriyar, and E. C, *Comparison of the efficiency of palladium and silver nanoparticles loaded on activated carbon and zinc oxide nanorods loaded on activated carbon as new adsorbents for removal of Congo red from aqueous solution: Kinetic and isotherm study*. 2012. **32**(4): p. 725-734.
36. MAHMOUD, D.K., *UTILIZATION OF BIOCHARS FROM WASTES OF THERMOCHEMICAL PROCESSES AS ADSORBENTS*. 2016.
37. Dawodu, F.A., K.G.J.J.o.m.r. Akpomie, and technology, *Simultaneous adsorption of Ni (II) and Mn (II) ions from aqueous solution unto a Nigerian kaolinite clay*. 2014. **3**(2): p. 129-141.

38. Weber, W., *JC Morris in: Proc. Int. Conf. Water Pollution Symposium, vol. 2*, 1962, Pergamon, Oxford.
39. Harikishore Kumar Re, D., S.-M. Lee, and K.J.E.E.R. Seshaiiah, *Removal of Cd (II) and Cu (II) from aqueous solution by agro biomass: equilibrium, kinetic and thermodynamic studies*. 2012. 17(3): p. 125-132.